Journal of Electronic Materials (2024) 53:5204–5211
https://doi.org/10.1007/s11664-024-11230-6

28TH INTERNATIONAL CONFERENCE ON NUCLEAR TRACKS AND RADIATION MEASUREMENTS

Effects of Lithium Ion Irradiation on Yttria-Stabilized Zirconia Thin Films: Structural and Optical Investigations

Praveen Gothwal[1] · Fouran Singh[2] · Vishnu Chauhan[3] · Bhawana Joshi[1]

Received: 15 March 2024 / Accepted: 30 May 2024 / Published online: 15 June 2024

Abstract

Thin films of yttria-stabilized zirconia (YSZ) were synthesized using spin coating technique on glass substrates with various concentration of yttria. The films were irradiated with Li^{3+} ions of energy 50 MeV and fluence values of 1×10^{11}, 5×10^{12} and 5×10^{13} ions/cm^2. The results obtained for the irradiated films are compared with the pristine sample. X-ray diffraction (XRD) was employed to confirm the structural phase and investigate the variation in crystallinity of irradiated thin films. X-ray diffraction analysis confirmed that the higher yttria concentrations corresponded to decrease in crystallinity in the zirconia, corroborated by calculated crystallite sizes. Interestingly, no phase formation was observed in sample YSZ (8%), highlighting the necessity of elevated annealing temperatures for phase formation, particularly at higher yttria concentrations. Significantly, the structural information was validated through Raman spectroscopy which revealed the decrease in the monoclinic phase with increasing yttria doping. The optical band gap of Zirconia increased with higher yttria doping concentration, resulting in a range of band gap from 4.11 eV to 4.15 eV. The exposure of YSZ thin films to Li^{3+} ions with an energy of 50 MeV unveiled impacts of ion fluence. Lower fluence levels resulted in observable damage to crystallinity when contrasted with pristine YSZ samples, as manifested by the broadening of diffraction peaks. At moderate fluence levels, a decrease in crystallinity damage was noted, nonetheless, at higher fluence levels, the damage intensified once more. The ion irradiation of YSZ (8%) resulted in the emergence and growth of crystalline phases.

Keywords YSZ thin film · ion irradiation · XRD · UV–visible · Raman spectroscopy

Introduction

Zirconia is a material that exists in the monoclinic phase at room temperature.[1,2] The monoclinic phase features a distorted fluorite structure with lattice parameters $a=514.6$ pm, $b=521.3$ pm, $c=531.1$ pm, and $\beta=99.2°$.[3] It undergoes a phase transition from monoclinic to tetragonal and then from tetragonal to cubic at elevated temperatures.[4] Among these phases, cubic zirconia is considered the most stable state, with a lattice parameter of $a=509$ pm. In general, the stability of cubic zirconia at room temperature can be achieved through doping with trivalent ions (Y^{3+}) or divalent ions (Ca^{2+}, Mg^{2+}), which function as stabilizers.[5,6] Among the mentioned stabilizers, Yttria-stabilized zirconia (YSZ) has been extensively researched both theoretically and experimentally because of its broad range of physical and chemical applications.[7–12] The Yttria stabilized zirconia is extensively utilized in various applications such as oxygen gas sensors where it serves as a sensing layer, as well as in thermal barrier coatings.[13–16] Additionally, it finds usage in solid oxide fuel cells, predominantly functioning as solid electrolytes.[17,18] Moreover, it is regarded as a promising material for hosting nuclear reactors.[19] In addition to these chemical methods of phase transformation and stabilization, ion beam irradiation is a prominent technique for inducing similar physical changes in the material's structure in a controlled manner.[3,12,20–22]

✉ Bhawana Joshi
bhawana@gbu.ac.in

[1] Department of Applied Physics, Gautam Buddha University, Greater Noida, Uttar Pradesh 201312, India

[2] Materials Sciences Group, Inter University Accelerator Centre, New Delhi 110067, India

[3] Department of Physics, Ramjas College, University of Delhi, New Delhi 110007, India

The fundamental applications of ion beams in materials science, encompassing both material modification and characterization, are driven by the interaction of energetic ions with matter. During its passage through a target material, an energetic incident ion continuously dissipates its energy through both elastic interactions as nuclear energy losses (S_n) and inelastic interactions as electronic energy losses (S_e) with the atoms of the material.[23] The mechanisms of nuclear and electronic energy losses are fundamentally distinct. Nuclear energy loss (S_n) predominates at low energies, around the keV range, leading to the creation of atomic-sized point defects, collision cascades with nuclei, and clusters of defects. In contrast, electronic energy loss (S_e) becomes dominant at high energies, in the MeV to GeV range.[23,24] The modifications induced are explained by the Thermal Spike and Coulomb Explosion models.[25,26] Numerous studies have documented the alterations in the physical and chemical properties of YSZ with low energy and high energy ion beam irradiation.[27–33] Ramola et al. observed that 120 MeV Ag^{9+} ion irradiation induces a phase transformation in pure zirconia from monoclinic to tetragonal, additionally, a transformation from the tetragonal phase to the cubic phase was observed in partially stabilized zirconia doped with yttria.[30] Parveen et al. investigated the impact of grain size and environmental temperature on radiation resistance. Their findings indicate that higher environmental temperatures contribute to enhanced radiation resistance.[27] The improvements in both mechanical properties and irradiation resistance were observed in CNTs/YSZ and graphene/YSZ nanocomposites.[34] Costantini et al. irradiated YSZ with electron energies ranging from 0.8 MeV to 2.5 MeV, noting that the dependence on electron energy leads to oxygen and zirconium vacancies.[35] Nanocrystalline ceramics exhibit greater radiation resistance compared to bulk materials due to the presence of a large volume fraction of grain boundaries and shorter diffusion distances.[21,36] The total volume of occupied grain boundaries in polycrystalline materials is dependent on the grain size, with an inverse relationship between the volume fraction of grain boundaries and the grain size.[21,37] Previous studies on the irradiation effects of nanocrystalline ZrO_2 and YSZ are subject to considerable disputed.[28,38–41] Additionally, in our research, we conducted irradiation experiments on Yttria-Stabilized Zirconia (YSZ) using lithium ions (Li^{3+}) having energy 50 MeV, investigating the influence of both Yttria concentration and ion fluence., while numerous studies have explored the effects of various energetic ion irradiations on yttria-stabilized zirconia, some for low energy ion irradiation where nuclear energy losses dominant and some for high energy irradiation where electronic energy losses dominant.[27,28,31,40,42–44] To the best of our knowledge, the impact of lithium ions with 50 MeV has yet to be investigated. Additionally, although there is extensive research on the fluence effect on fully stabilized YSZ, there is a notable scarcity of studies examining the effects of different concentrations of yttria.[30,45] Hence, it's crucial to explore how the structure and optical characteristics of the material respond under intense irradiation. This investigation holds significant implications for the practical utilization of YSZ, especially in demanding environments like space exploration, nuclear industries, and radiation zones.[10,46,47]

Experimental Details

The precursors utilized for synthesis of YSZ included $ZrO(NO_3)_2{\cdot}xH_2O$ (zirconium nitrate hydrate) and $(YNO_3)_3.6H_2O$ (yttrium nitrate hexahydrate). Additionally, citric acid was used to facilitate gel formation. Pure zirconia, along with yttria-doped zirconia at concentrations of 4 mol.% and 8 mol.%, were synthesized using varying weights of precursors and the synthesized samples are named as YSZ (0%), YSZ (4%) and YSZ (8%) respectively. To begin, separate solutions were created for each precursor. $ZrO(NO_3)_2{\cdot}xH_2O$ was dissolved in water to obtain the zirconia precursor solution, while $(YNO_3)_3{\cdot}6H_2O$ was dissolved in water to form the yttrium precursor solution. Simultaneously, a solution of citric acid was prepared by dissolving it in water. In the subsequent step, the yttrium solution was gradually added drop wise into the zirconia solution while stirring the mixture continuously. This controlled addition allowed for the proper incorporation of yttrium into the zirconia matrix, which is essential for yttria stabilization. To facilitate the formation of a gel-like structure, the citric acid solution was introduced into the yttria-stabilized zirconia mixture while stirring at a controlled temperature of 60°C. The resulting solution was then stirred at 60°C for a duration of 30 min to ensure homogenization and the formation of a uniform gel. The gel was then subjected to a drying process by gradually raising the temperature to 100°C, causing the water within the gel to vaporize. Once a uniform gel was obtained, the heat source was removed, signifying the completion of the drying process. The prepared gel was subsequently utilized for the deposition of thin films using the spin coater (SpinNXG-P1A). A glass substrate was selected as the substrate, onto which the gel was dispensed at the center while the glass substrate was securely mounted on the spin coater chuck. The optimal condition for achieving a uniform and smooth film was determined to be 3000 rpm (rotations per minute) for duration of 1 min. Following the above procedure, the samples were annealed at 500°C for 4 h in a furnace to achieve the desired structural phase formation. These pristine samples were characterized using x-ray diffraction (Rigaku Miniflex), Raman spectroscopy and UV–visible spectroscopy. The samples underwent

irradiation with high energy at three distinct fluence levels to investigate the dominant electronic energy loss in YSZ material. The samples underwent irradiation by Li^{3+} ions with an energy of 50 MeV at the Inter-university Accelerator Centre (IUAC) in New Delhi. In this study, we investigated the effect of three distinct fluence levels: 1×10^{11} ions/cm^2 (low fluence), 5×10^{12} ions/cm^2 (medium fluence), and 5×10^{13} ions/cm^2 (high fluence) on the synthesized YSZ thin films. Subsequently, the irradiated sample was subjected to characterization using x-ray diffraction, Raman spectroscopy, and UV–visible spectroscopy. The obtained results were then compared with those of the pristine sample.

Results and Discussion

Characterization of Pristine YSZ

X-ray Diffraction

X-ray diffraction spectra were obtained for pristine YSZ (0%), YSZ (4%), and YSZ (8%), within a 2θ value range of 20° to 80°. The peak positions for (111), (200), (220), and (311) were observed at 30.94°, 35.5°, 51.12°, and 60.4° respectively. X-ray diffraction spectra were obtained for pristine pure zirconia, YSZ (4%) and YSZ (8%) are depicted in Fig. 1. The peak positions observed in the spectra confirmed the presence of the tetragonal phase (JCPDS-80-0965), also compared with reported results.[28,30,48] The average crystallite size (D) of YSZ samples was determined employing the Debye–Scherrer equation:

$$D = \frac{k\lambda}{\beta\cos\theta}$$

where k represents the shape factor (assumed as 0.9 for spherical particles), λ denotes the x-ray wavelength (1.5406 Å), β signifies the full width at half maximum (FWHM) value of the diffraction peak (in radians), and θ stands for the Bragg angle.[49] The crystallite size of (111) peak was calculated to be 10.22 nm for pure Zirconia, 6.41 nm for YSZ (4%), and no phase formation was observed for YSZ (8%). Additionally, a decrease in crystallinity was observed as the concentration of yttria increased in the zirconia. A increment in FWHM is observed with an increase in yttria concentration. Since crystallinity is inversely related to FWHM, this indicates that crystallinity decreases for higher yttria concentration. Additionally, the crystallite size measurements confirm the nanocrystalline structure of YSZ. These findings suggest that higher concentrations of yttria necessitate elevated annealing temperatures for phase formation.

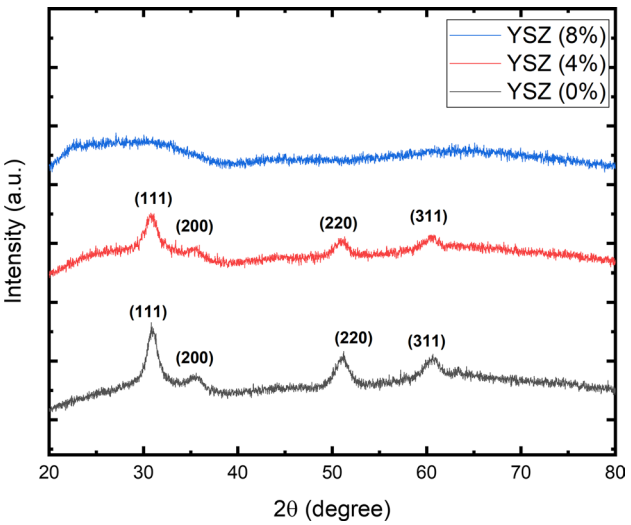

Fig. 1 X-ray diffraction spectra of pristine YSZ with different concentration of Yttria

Raman Spectroscopy

The XRD analysis successfully confirmed the phase for pure Zirconia and 4% YSZ, but was unable to confirm the phase for YSZ (8%) likely due to inadequate annealing temperature. To ascertain the phase of YSZ (8%), Raman spectroscopy was employed. Zirconia demonstrates various symmetries in its crystal structure. In the monoclinic symmetry, each unit cell contains four molecules, exhibiting eighteen Raman active modes. This characteristic is clearly observed in the Raman spectra of YSZ (0%), conversely, zirconia's tetragonal symmetry configuration comprises two molecules within each unit cell, resulting in six Raman active modes. This pattern is consistent across doped spectra, except for pure Zirconia as shown in Fig. 2 and justified with other significant reported results.[31] The formation of B_{1g} and E_g bonds are presented in Fig. 2. From this, it is concluded that YSZ (0%) contains both tetragonal and monoclinic phases, whereas doped Zirconia only contains the tetragonal phase. Further, with increasing the doping concentration, the number of peaks are decreased which is similarly justified using the XRD results.

UV–Visible Spectroscopy

UV–visible spectroscopy was utilized to investigate the optical properties of YSZ thin films deposited at varying concentrations of Yttria in Zirconia, namely YSZ (0%), YSZ (4%), YSZ (8%). The films were assessed in the UV–visible range

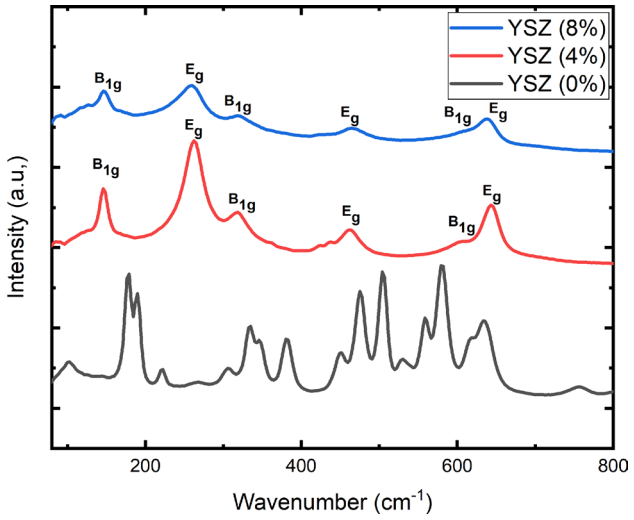

Fig. 2 Raman spectra of YSZ with three different concentrations of Yttria doping.

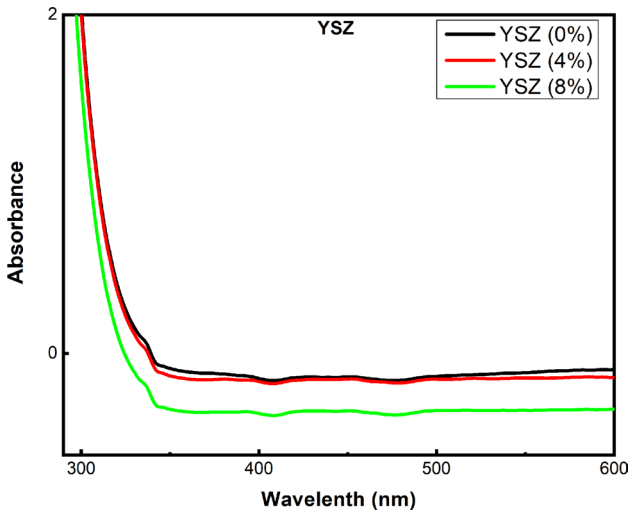

Fig. 3 UV Visible spectra of absorbance with wavelength for various concentration of Yttria in Zirconia.

to analyze their absorption characteristics as shown in Fig. 3. Absorbance spectra were recorded across the UV to visible light wavelengths to examine how film thickness and YSZ concentration influence their optical behavior as observed in previous literature.[50] Typically, oxides exhibit absorbance curves rather than sharp peaks. These absorbance curves serve as a basis for determining the optical band gap of the material. In our study, we utilized UV–visible spectroscopy to plot the absorbance curve of YSZ. The optical band gap was then calculated through the Tauc's plot analysis of the absorbance curve. This analysis not only determines the band gap but also provides insights into whether the band structure is direct or indirect. In our investigation, the band

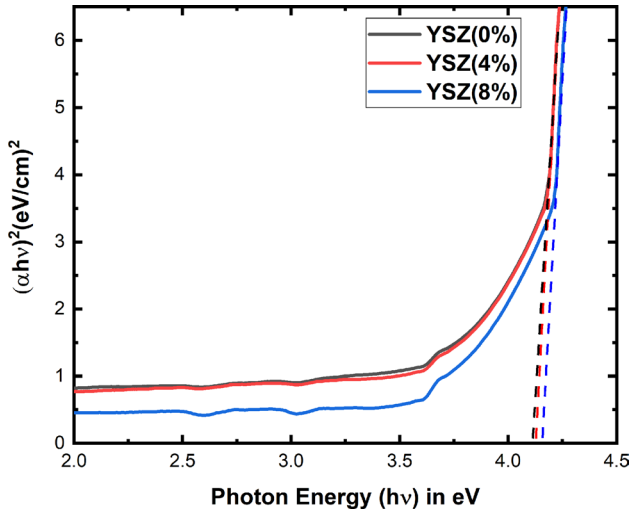

Fig. 4 Tauc's plot of YSZ to determine the direct band gap values at different concentration of yttria.

gap of YSZ falls within the range of 4.11 to 4.15, as determined by the Tauc's plot analysis.[51] It was observed that the band gap of Zirconia increased with higher yttria doping percentages as shown in Fig. 4. The variation in band gap value differs slightly due to change in the crystallite size of the same samples.

Result and Discussion for Irradiated YSZ and Comparison with Pristine

X-ray Diffraction

The thin films of YSZ were irradiated with Li^{3+} ions at an energy of 50 MeV. The three different low, medium and high fluence were applied having values 1×10^{11} ions/cm^2, 5×10^{12} ions/cm^2 and 5×10^{13} ions/cm^2 respectively during the irradiation process. The XRD characterization was performed to analyze the structural changes induced by ion irradiation. The results were compared with pristine YSZ samples to assess the extent of change in crystallinity other parameters.[48] The XRD analysis revealed notable effects of ion fluence on pure Zirconia or YSZ (0%). At low ion fluence levels, there was a damage to crystallinity in comparison to pristine YSZ samples. This damage manifested as broadening of diffraction peaks. As the ion fluence increased to medium levels, there was a reduction in crystallinity damage, suggesting potential annealing or recovery effects. However, at higher fluence levels, the damage to crystallinity intensified once again, indicating saturation or surpassing of recovery mechanisms. The slight variation is observed in intensity of the peaks with increasing the fluence as compared with the pristine sample, as presented in Fig. 5. It is

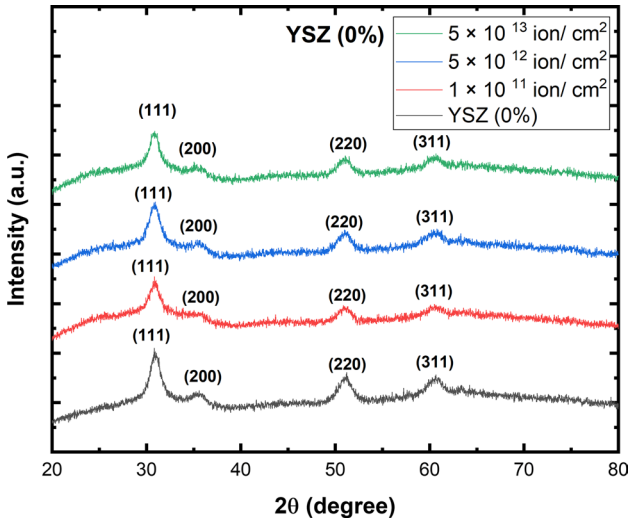

Fig. 5 X-ray diffraction spectra of YSZ (0%) and irradiated samples with different fluence.

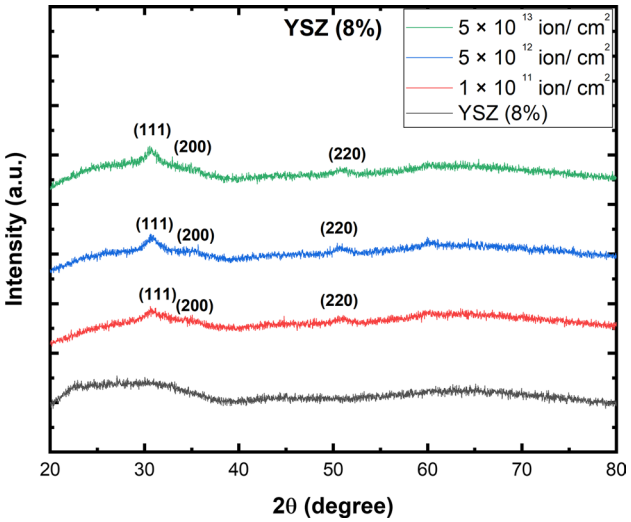

Fig. 7 X-ray diffraction spectra of YSZ (8%) and irradiated samples with different fluence.

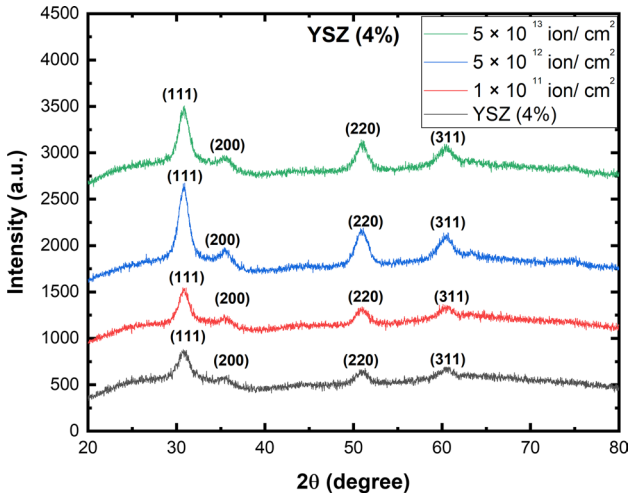

Fig. 6 X-ray diffraction spectra of YSZ (4%) and irradiated samples with different fluence.

observed that the diffraction peaks (111), (200), (220) and (311) which confirm the presence of tetragonal structure.

Again, at low ion fluence levels, there was noticeable crystallinity damage compared to pristine YSZ (4%) samples. As the ion fluence increased to medium levels, a reduction in crystallinity damage was observed. However, with further escalation of ion fluence, the damage to crystallinity intensified once again. The crystallinity damage in YSZ (4%) with an initial decrease followed by an increase in damage with increasing fluence. As shown in Fig. 6, it is observed that the intensity of the peaks increased and sharpen with increasing ion fluence as compared to the pristine YSZ (4%). It is resulted that the crystallinity is improved with improvement in peak intensity. Similarly, in ion irradiation of YSZ (8%), there was an evident emergence and growth of crystalline phases as shown in Fig. 7. However, as the ion fluence increased to high ion fluence, there was notable damage in crystallinity compared to the medium ion fluence condition. This observation indicates a correlation between ion fluence and the emergence, growth, and subsequent damage of crystalline phases in YSZ (8%). The intensity of the peaks is increased up to the fluence of 5×10^{12} ions/cm^2 and further decreased at higher fluence. The obtained results revealed that the significant change is observed in structural properties under the effect of ion irradiation at different fluence. The FWHM of the (111) peak was measured to be 0.84° for the pristine sample, 0.89° for the low fluence sample, 0.87° for the medium fluence sample, and 0.88° for the high fluence sample for YSZ(0%). Correspondingly, the crystallite sizes were determined to be 10.22 nm for pristine, 9.68 nm for low fluence, 9.9 nm for medium fluence, and 9.79 nm for high fluence. For YSZ (4%), the FWHM of the (111) peak is measured as follows: 1.343° for the pristine sample, 1.35° for low fluence, 1.3° for medium fluence, and 1.33° for high fluence. The corresponding crystallite sizes are 6.41 nm for the pristine sample, 6.38 nm for low fluence, 6.63 nm for medium fluence, and 6.48 nm for high fluence. For YSZ (8%), the FWHM of the (111) peak was observed to be 3.22° for low fluence, 1.48° for medium fluence, and 1.57° for high fluence, correspondingly, the crystallite sizes were determined to be 2.69 nm, 5.82 nm, and 5.49 nm for low, medium, and high fluences, respectively. The variation in FWHM of peak (111) with fluence is shown in Fig. 8.

X-ray diffraction analysis of YSZ (0%), and YSZ (4%) confirm the presence of the tetragonal phase. Notably, an inverse relationship was observed between yttria

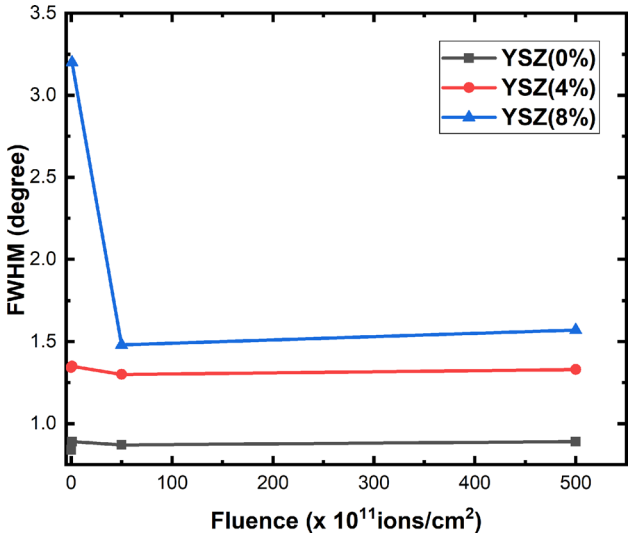

Fig. 8 Variation in the FWHM of peak (111) with fluence.

concentration and crystallinity, with higher yttria concentrations leading to decreased crystallinity in the zirconia. The calculated average crystallite sizes corroborated this trend, with pure Zirconia exhibiting the largest crystallite size, followed by YSZ (4%) with a smaller size, and no observable phase formation in YSZ (8%). These results underscore the importance of elevated annealing temperatures for phase formation, particularly at higher yttria concentrations. To address the phase of YSZ (8%), Raman spectra were employed, revealing insights into the crystal structure of Zirconia. The Raman spectra of YSZ suggests that YSZ (0%) contains both tetragonal and monoclinic phases, while doped Zirconia predominantly consists of the tetragonal phase. The band gap of Zirconia increased with higher yttria doping percentages. This resulted in a range of band gap values spanning from 4.11 eV to 4.15 eV. Zirconia undergoes phase transitions from monoclinic to tetragonal and then to cubic as the temperature increases. At room temperature, zirconia is naturally in the monoclinic phase. Although the cubic phase is considered the most stable and desirable for many applications, it is not typically present at room temperature. However, doping with yttria allows the stabilization of the cubic phase at room temperature. Typically, a 4% molar concentration of yttria transforms the monoclinic phase of zirconia into the tetragonal phase, resulting in partially stabilized YSZ. In contrast, an 8% molar concentration of yttria converts the monoclinic phase of zirconia into the cubic phase, producing fully stabilized YSZ. In this work, we successfully achieved this stable phase, demonstrating significant radiation tolerance in the material. Typically, bulk YSZ is found in the monoclinic phase at room temperature. However, Kalita et al.[48] observed that pure zirconia thin films exhibit a stable phase.[33] The same stable phase was observed in the XRD spectra of YSZ (0%) thin film. Furthermore, the reduction in peak intensity was noticed with increasing yttria concentration. This reduction is likely due to the higher annealing temperatures required for higher yttria concentrations. This observation is supported by irradiation experiments on the YSZ (8%) thin film. The exposure of YSZ thin films to Li^{3+} ions at an energy of 50 MeV unveiled impacts of ion fluence. Post-irradiation, the crystallinity of this film increased, indicating that the higher yttria concentration required higher annealing temperatures to achieve optimal crystallinity. Lower fluence levels resulted in observable damage to crystallinity when contrasted with pristine YSZ samples, as manifested by the broadening of diffraction peaks. At moderate fluence levels, a decrease in crystallinity damage was noted, suggesting potential annealing or recovery effects. Nonetheless, at higher fluence levels, the damage intensified once more. The ion irradiation of YSZ (8%) resulted in the emergence and growth of crystalline phases. However, as the ion fluence increased to high levels, significant damage to crystallinity was observed compared to the medium ion fluence condition.

Conclusion

X-ray diffraction analysis revealed the tetragonal phase in YSZ (0%) and YSZ (4%), with higher yttria concentrations correlating to decreased crystallinity. Raman spectra indicated that YSZ (0%) contains both tetragonal and monoclinic phases, while doped Zirconia predominantly consists of the tetragonal phase. The band gap of Zirconia increased with higher yttria doping percentages ranging from 4.11 eV to 4.15 eV. Exposure to Li^{3+} ions at 50 MeV showed fluence-dependent damage to crystallinity, ion fluence impacts were evident, with lower fluence levels causing crystallinity damage, but damage decrease at medium fluence and again high fluence intensifying damage. Ion irradiation of YSZ (8%) led to crystalline phase emergence, but high fluence levels resulted in significant crystallinity damage compared to moderate levels.

Acknowledgments One of the authors (Praveen Gothwal) is thankful to the Council of Scientific and Industrial Research (CSIR) for providing Junior Research Fellowship (CSIR-JRF) under file number 09/1013(0014)2021-EMR-I, for conducting this research work. Authors (P. Gothwal and B. Joshi) are thankful to Inter University Accelerator Centre (IUAC), New Delhi, India for providing the Beam time and access to High Energy Beam Facility.

Author Contributions Praveen Gothwal: Conceptualization, Methodology, Validation, Formal analysis, Investigation. Fouran Singh: Visualization and monitoring of analysis. Vishnu Chauhan: Conceptualization and Visualization. Bhawana Joshi: Manuscript drafting, Monitoring of overall study.

Conflict of interest The authors declare that they have no conflict of interest.

References

1. N. Claussen, M. Ruhle, and A.H. Heuer, *Science and Technology of Zirconia II* (New York: American Ceramic Society Inc, 1983).
2. R. Stevens, *Zirconia and Zirconia Ceramics*, 2nd ed., (Twickenham: Magnesium Elektron, 1986).
3. K.E. Sickafus, H.J. Matzke, T.H. Hartmann, K. Yasuda, J.A. Valdez, P. Chodak III., M. Nastasi, and R.A. Verrall, Radiation damage effects in zirconia. *J. Nucl. Mater.* 274, 66 (1999).
4. R.H. French, S.J. Glass, F.S. Ohuchi, Y.N. Xu, and W.Y. Ching, Experimental and theoretical determination of the electronic structure and optical properties of three phases of ZrO_2. *Phys. Rev. B* 49, 5133 (1994).
5. S. Nath, S. Bajaj, and B. Basu, Microwave-sintered MgO-doped zirconia with improved mechanical and tribological properties. *Int. J. Appl. Ceram. Technol.* 5, 49 (2008).
6. N.S. Jacobson, Z. Liu, L. Kaufman, and F. Zhang, Thermodynamic modeling of the $YO_{1.5}$–ZrO_2 system. *J. Am. Ceram. Soc.* 87, 1559 (2004).
7. L. Combemale, G. Caboche, D. Stuerga, and D. Chaumont, Microwave synthesis of yttria stabilized zirconia (YSZ). *Mater. Res. Bull.* 40, 529 (2005).
8. C.W. Kuo, Y.H. Lee, I.M. Hung, M.C. Wang, S.B. Wen, K.Z. Fung, and C.J. Shih, Crystallization kinetics and growth mechanism of 8 mol.% yttria-stabilized zirconia (8YSZ) nano-powders prepared by a sol-gel process. *J. Alloys Compd.* 453, 470 (2008).
9. J. Molina Reyes, H. Tiznado, G. Soto, M. Vargas-Bautista, D. Dominguez, E. Bracamontes, D. Sweeney, and J. Read, Physical and electrical characterization of yttrium-stabilized zirconia (YSZ) thin films deposited by sputtering and atomic-layer deposition. *J. Mater. Sci. Mater. Electron.* 29, 15349 (2018).
10. J.C. Ray, R.K. Pati, and P. Pramanik, Chemical synthesis and structural characterization of nanocrystalline powders of pure zirconia and yttria stabilized zirconia (YSZ). *J. Eur. Ceram. Soc.* 20, 1289 (2000).
11. S. Tailor, M. Singh, and A. Doub, Synthesis and characterization of yttria-stabilized zirconia (YSZ) nano-clusters for thermal barrier coatings (TBCs) applications. *J. Clust. Sci.* 27, 1097 (2016).
12. L. Chen, Y. Chang, Q. Guo, J. Zhang, F. Wan, and Y. Long, Phase stability, grain growth and photoluminescence property of nanocrystalline yttria-stabilized zirconia film under 500 keV Xe^{6+} ion irradiation. *Nucl. Instrum. Methods Phys. Res. Sect. B* 328, 84 (2014).
13. S. Akasaka, Y. Amamoto, H. Yuji, and I. Kanno, Limiting current type yttria-stabilized zirconia thin-film oxygen sensor with spiral Ta_2O_5 gas diffusion layer. *Sens. Actuat. B Chem.* 327, 128932 (2021).
14. M. Raza, D. Cornil, J. Cornil, S. Lucas, R. Snyders, and S. Konstantinidis, Oxygen vacancy stabilized zirconia (OVSZ); a joint experimental and theoretical study. *Scripta Mater.* 124, 26 (2016).
15. Y.H. Lee, C.W. Kuo, I.M. Hung, K.Z. Fung, and M.C. Wang, The thermal behavior of 8 mol.% yttria-stabilized zirconia nanocrystallites prepared by a sol-gel process. *J. Non-Cryst. Solids* 351, 3709 (2005).
16. A.M. Adamska, R. Springell, A.D. Warren, L. Picco, O. Payton, and T.B. Scott, Growth and characterization of uranium-zirconium alloy thin films for nuclear industry applications. *J. Phys. D Appl. Phys.* 47, 10 (2014).
17. S. de Souza, S.J. Visco, and L.C. De Jonghe, Thin-film solid oxide fuel cell with high performance at low-temperature. *Solid State Ion.* 98, 57 (1997).
18. R. Frison, S. Heiroth, J.L.M. Rupp, K. Conder, E.J. Barthazy, E. Müller, M. Horisberger, M. Döbeli, and L.J. Gauckler, Crystallization of 8 mol.% yttria-stabilized zirconia thin-films deposited by RF-sputtering. *Solid State Ion.* 232, 29 (2013).
19. Y.W. Lee, C.Y. Joung, S.H. Kim, and S.C. Lee, Inert matrix fuel—a new challenge for material technology in the nuclear fuel cycle. *Met. Mater. Int.* 7, 159 (2001).
20. G. Ackland, Controlling radiation damage. *Science* 327, 1587 (2010).
21. I.J. Beyerlein, A. Caro, M.J. Demkowicz, N.A. Mara, A. Misra, and B.P. Uberuaga, Radiation damage tolerant nanomaterials. *Mater. Today* 16, 443 (2013).
22. J. Adam and B. Cox, The irradiation-induced phase transformation in zirconia solid solutions. *J. Nucl. Energy Part A React Sci.* 11, 31 (1959).
23. M. Nastasi and J.W. Mayer, *Ion Implantation and Synthesis of Materials* (Berlin: Springer, 2006).
24. S.J. Zinkle and V.A. Skuratov, Track formation and dislocation loop interaction in spinel irradiated with swift heavy ions. *Nucl. Instrum. Methods Phys. Res. Sect. B* 141, 737 (1998).
25. N. Itoh, D.M. Duffy, S. Khakshouri, and A.M. Stoneham, Making tracks: electronic excitation roles in forming swift heavy ion tracks. *J. Phys. Condens. Matter* 21, 474205 (2009).
26. J.-M. Costantini, C. Trautmann, L. Thomé, J. Jagielski, and F. Beuneu, Swift heavy ion-induced swelling and damage in yttria-stabilized zirconia. *J. Appl. Phys.* 101, 073501 (2007).
27. R. Parveen, P. Kalita, R. Shukla, V. Grover, R. Pandey, G. Sattonnay, and D.K. Avasthi, Investigation of radiation tolerance of yttria stabilized zirconia in the ballistic collision regime: effect of grain size and environmental temperature. *Nucl. Instrum. Methods Phys. Res. Sect. B* 551, 165344 (2024).
28. S. Dey, J.W. Drazin, Y. Wang, J.A. Valdez, T.G. Holesinger, B.P. Uberuaga, and R.H.R. Castro, Radiation tolerance of nanocrystalline ceramics: insights from yttria stabilized zirconia. *Sci. Rep.* 5, 7746 (2015).
29. P. Kalita, S. Ghosh, G. Sattonnay, U.B. Singh, I. Monnet, and D.K. Avasthi, Radiation response of nano-crystalline cubic zirconia: comparison between nuclear energy loss and electronic energy loss regimes. *Nucl. Instrum. Methods Phys. Res. Sect. B* 435, 19 (2018).
30. R.C. Ramola, M. Rawat, K. Joshi, A. Das, S.K. Gautam, and F. Singh, Study of phase transformation induced by electronic excitation in pure and yttrium doped ZrO_2 thin films. *Mater. Res. Express* 4, 096401 (2017).
31. T. Hojo, J. Aihara, K. Hojou, S. Furuno, H. Yamamoto, N. Nitani, T. Yamashita, K. Minato, and T. Sakuma, Irradiation effects on yttria-stabilized zirconia irradiated with neon ions. *J. Nucl. Mater.* 319, 81 (2003).
32. T. Hojo, H. Yamamoto, J. Aihara, S. Furuno, K. Sawa, T. Sakuma, and K. Hojou, Radiation effects on yttria-stabilized zirconia irradiated with He or Xe ions at high temperature. *Nucl. Instrum. Methods Phys. Res. Sect. B* 241, 536 (2005).
33. N. Sasajima, T. Matsui, K. Hojou, S. Furuno, H. Otsu, K. Izui, and T. Muromura, Radiation damage in yttria-stabilized zirconia under Xe ion irradiation. *Nucl. Inst. Methods Phys. Res. B* 141, 487 (1998).
34. X. Zhang, C. Sun, H. Ji, M. Yang, H. Zhang, W. Tian, Y. Wu, O.V. Tolochko, and Y. Wang, A review of CNTs and graphene reinforced YSZ nanocomposites: preparation, mechanical and anti-irradiation properties. *J. Mater. Sci. Technol.* 167, 27 (2023).
35. J.-M. Costantini, O. Cavani, and B. Boizot, On-line optical absorption of electron-irradiated yttria-stabilized zirconia. *J. Phys. Chem. Solids* 169, 110853 (2022).

36. X.-M. Bai, A.F. Voter, R.G. Hoagland, M. Nastasi, and B.P. Uberuaga, Efficient annealing of radiation damage near grain boundaries via interstitial emission. *Science* 327, 1631 (2010).
37. K.E. Sickafus, L. Minervini, R.W. Grimes, J.A. Valdez, M. Ishimaru, F. Li, K.J. McClellan, and T. Yamashita, Radiation tolerance of complex oxides. *Science* 289, 748 (2000).
38. A. Debelle, J.-P. Crocombette, A. Boulle, E. Martinez, B.P. Uberuaga, D. Bachiller-Perea, Y. Haddad, F. Garrido, L. Thomé, and M. Béhar, How relative defect migration energies drive contrasting temperature-dependent microstructural evolution in irradiated ceramics. *Phys. Rev. Mater.* 2, 083605 (2018).
39. C. Onofri, C. Sabathier, H. Palancher, G. Carlot, S. Miro, Y. Serruys, L. Desgranges, and M. Legros, Evolution of extended defects in polycrystalline UO_2 under heavy ion irradiation: combined TEM, XRD and Raman study. *Nucl. Instrum. Methods Phys. Res. Sect. B* 374, 51 (2016).
40. P. Kalita, S. Ghosh, U.B. Singh, P.K. Kulriya, V. Grover, R. Shukla, A.K. Tyagi, G. Sattonnay, and D.K. Avasthi, Investigating the effect of material microstructure and irradiation temperature on the radiation tolerance of yttria stabilized zirconia against high energy heavy ions. *J. Appl. Phys.* 125, 115902 (2019).
41. V. Chauhan, D. Gupta, N. Koratkar, and R. Kumar, Phase transformation and enhanced blue photoluminescence of zirconium oxide poly-crystalline thin film induced by Ni ion beam irradiation. *Sci. Rep.* 11, 17672 (2021).
42. T. Hojo, H. Yamamoto, J. Aihara, S. Furuno, K. Sawa, T. Sakuma, and K. Hojou, Loop formation by ion irradiation in yttria stabilized zirconia. *Nucl. Instrum. Methods Phys. Res. Sect. B* 250, 101 (2006).
43. A.P. Caricato, A. Lamperti, P.M. Ossi, C. Trautmann, and L. Vanzetti, Modifications of yttria fully stabilized zirconia thin films by ion irradiation in the inelastic collision regime. *J. Appl. Phys.* 104, 093534 (2008).
44. F. Garrido, S. Moll, G. Sattonnay, L. Thomé, and L. Vincent, Radiation tolerance of fluorite-structured oxides subjected to swift heavy ion irradiation. *Nucl. Instrum. Methods Phys. Res. Sect. B* 267, 1451 (2009).
45. V. Kulyk, Z. Duriagina, A. Kostryzhev, B. Vasyliv, V. Vavrukh, and O. Marenych, The effect of yttria content on microstructure, strength, and fracture behavior of yttria-stabilized zirconia. *Materials* 15, 5212 (2022).
46. V. Chauhan, T. Gupta, N. Koratkar, and R. Kumar, Studies of the electronic excitation modifications induced by SHI of Au ions in RF sputtered ZrO_2 thin films. *Mater. Sci. Semicond. Process.* 88, 262 (2018).
47. V. Chauhan, T. Gupta, P. Singh, P.D. Sahare, N. Koratkar, and R. Kumar, Influence of 120 MeV S^{9+} ion irradiation on structural, optical and morphological properties of zirconium oxide thin films deposited by RF sputtering. *Phys. Lett. A* 383, 898 (2019).
48. P. Kalita, S. Ghosh, G. Sattonnay, U.B. Singh, V. Grover, R. Shukla, S. Amirthapandian, R. Meena, A.K. Tyagi, and D.K. Avasthi, Role of temperature in the radiation stability of yttria stabilized zirconia under swift heavy ion irradiation: a study from the perspective of nuclear reactor applications. *J. Appl. Phys.* 122, 025902 (2017).
49. L. Alexander and H.P. Klug, Determination of crystallite size with the x-ray spectrometer. *J. Appl. Phys.* 21, 137 (1950).
50. M. Ramazanov, F. Hajiyeva, and H. Shirinova, Fabrication, characterization and optical properties of transparent PP/Yttria-stabilized zirconia (YSZ) based nanocomposites. *J. Elastomers Plast.* 53, 417 (2021).
51. J. Tauc, R. Grigorovici, and A. Vancu, Optical properties and electronic structure of amorphous germanium. *Phys. Status Solidi B* 15, 627 (1966).